Journal of the Optical Society of Korea
Vol. 16, No. 1, March 2012, pp. 17-21

DOI: http://dx.doi.org/10.3807/JOSK.2012.16.1.017

Photopolymer-based Surface-normal Input/Output Volume Holographic Grating Coupler for 1550-nm Optical Wavelength

Kwon-Yeon Lee[1]*, Sang-Huek Jeung[1], Byung-Mo Cho[1], and Nam Kim[2]

[1]Department of Electronic Engineering, Sunchon National University, Sunchon 540-742, Korea
[2]Department of Computer and Communication, Chungbuk National University, Cheongju 361-763, Korea

(Received November 15, 2011 : revised January 3, 2012 : accepted January 4, 2012)

A surface-normal input/output volume holographic grating coupler (VHGC) operating at 1550nm wavelength region by using a 10μm-thick DuPont photopolymer film is designed and fabricated. The angular and wavelength responses of the input/output VHGC are investigated in order to validate applicability of this device in integrated optics and optical communications. The effect of incident-beam position on the output reflectance to determine optimum condition for input coupling is also presented. The fabricated input/output VHGC exhibited an angular selectivity of ~0.027°, a wavelength selectivity of ~0.8 nm, and an output peak reflectance of 34.13%.

Keywords : Holographic optical elements, Volume holographic grating, Waveguide couplers
OCIS codes : (090.2890) Holographic optical elements; (090.7330) Volume holographic gratings; (060.1810) Buffers, couplers, routers, switches, and multiplexers

I. INTRODUCTION

Photopolymer-based input/output volume holographic grating couplers (VHGCs) are attractive elements for coupling lights into and out from waveguides in the field of integrated optics and optical communication applications. Unlike other types of devices used as couplers for optical waveguides -i.e. prism couplers, reflective couplers, and surface-relief grating couplers-, VHGC provides relatively higher coupling efficiency and preferential-order coupling characteristics, and can be fabricated through a dry process at low cost. Because of these advantageous features adaptable to diverse applications of VHGCs, many researchers have proposed various numerical approaches to formulate their characteristics [1-4]. Recently, we have proposed and theoretically investigated an input/output coupler system using volume holographic gratings to achieve high-efficiency coupling with respect to the Bragg-angle mismatch and the index modulation at 1550nm wavelength [5]. The outstanding angular and wavelength selectivity of common reflection-type volume holographic gratings that result from the Bragg effect are expected to make possible a sharp angular and wavelength selective coupling in a VHGC,. This is an advantageous characteristic applicable to wavelength division multiplexing (WDM) systems. The wavelength response of an output VHGC with respect to the index modulation, the waveguide index, and grating thickness, have been analyzed by Villalaz et al. for coarse wavelength division multiplexing (CWDM) system applications [6]. However, there has been a limited experimental demonstration and an analysis to investigate the angular and wavelength responses for the structure of both input and output grating couplers embedded in the waveguide film, this type of coupler may be called an input/output VHGC [7-9].

In this paper, we present the experimental and theoretical study on the angular and spectral responses of the surface-normal input/output VHGC operating at 1550 nm wavelength region. The input/output VHGC is implemented by using a 10μm-thick DuPont photopolymer HRF600×123-10, which is a high performance holographic film used for transmission and reflection gratings.

II. DESIGN AND FABRICATION

The basic configuration of the input/output VHGC for a surface-normal input-output coupling is shown in Fig. 1. The input/output VHGC consists of a photopolymer waveguide

*Corresponding author: kwonyeon@sunchon.ac.kr
Color versions of one or more of the figures in this paper are available online.

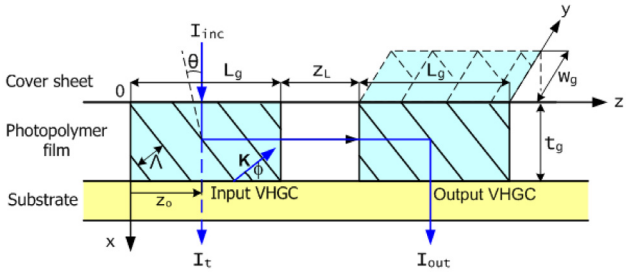

FIG. 1. Input/output VHGC configuration. The VHGC is composed of an input coupler, a waveguide, and an output coupler. The incident intensity of the input beam is I_{inc}, while I_t and I_{out} denote the intensity of the transmitted beam and the intensity of the output beam respectively, for the specific coupling angle. z_o is the position of the incident input beam on the surface of the input VHGC, and w_g is the width of the grating.

film, a glass substrate, and a cover sheet. Two VHGCs with gratings of the same length L_g and thickness t_g are embedded in the photopolymer film wherein, two couplers are separated by a waveguide of length z_L. The photopolymer film acts as both the grating medium and the waveguide layer. In this paper, the two couplers are of identical volume phase gratings with ϕ=45° slanted angle, so the grating vector $\mathbf{K}$ of the two VHGCs have the same magnitude of $|\mathbf{K}|=2\pi/\Lambda$ (Λ is the grating period.). A surface-normal-incident input beam is 90° diffracted into the plane of the waveguide by an input VHGC and is guided toward the output VHGC through the waveguide. The guided beam is then 90° diffracted by an output VHGC, therefore the output beam is shifted laterally with respect to the input beam.

To meet the Bragg condition, the grating period Λ must satisfy [10]

$$\Lambda=\lambda_r/2n_{gr}\cos(\phi-\theta), \quad (1)$$

where λ_r is the wavelength of the incident beam in free-space, n_{gr} is the average refractive index of the grating, ϕ is the slant angle of the grating, and θ is the incidence angle of the input beam in the photopolymer. With parameters n_{gr}=1.49, ϕ=45°, and θ=0°, we have a grating period Λ=~0.7355μm at 1550nm readout wavelength. In order to fabricate couplers with a 45° slanted volume phase grating into the photopolymer film, the interferometric recording configuration including a prism-pair shown in Fig. 2 is applied. The HRF600×123-10 photopolymer with t_g=10μm is laminated onto a fused-silica glass substrate with a dimensions of 85mm×25mm×1.5mm after one of the Mylar cover sheets is removed. The dimensions of a fused-silica prism were of 60mm×60mm×25mm, and the prisms were antireflection coated to reduce reflections. The prism system is placed on a motorized rotation stage, and the rotation stage is mounted on the 2-axis translation stages to position accurately the recording beams inside the photopolymer film. From the geometry of the prism and Snell's

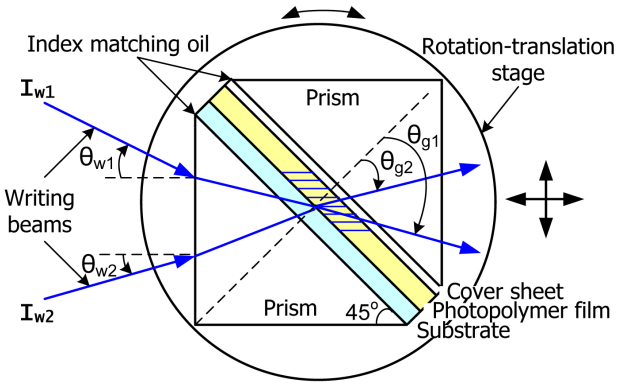

FIG. 2. Experimental setup for recording input/output VHGC.

law, the recording angles at the air-prism interface can be written as

$$\theta_{w1}=\sin^{-1}\left[n_{pw}\sin\left\{\sin^{-1}\left[(n_{gw}/n_{pw})\sin\theta_{g1}\right]-45^{\circ}\right\}\right], \quad (2a)$$

$$\theta_{w2}=\sin^{-1}\left[n_{pw}\sin\left\{45^{\circ}-\sin^{-1}\left[(n_{gw}/n_{pw})\sin\theta_{g2}\right]\right\}\right], \quad (2b)$$

where n_{pw} and n_{gw} are the refractive indices of a fused-silica 45°-45°-90° prism and a photopolymer film at recording wavelength λ_w respectively, $\theta_{g1,g2}=\phi_o\pm\sin^{-1}\left[\lambda_w/2n_{gw}\Lambda_o\right]$ are the beam angles inside the photopolymer, ϕ_o is the grating slanted angle, and $\Lambda_o=\lambda_w/2n_{gw}\sin\left[(\theta_{g1}-\theta_{g2})/2\right]$ is the grating period. In our recording configuration, the material shrinkage of the photopolymer [11] should be considered in the calculation of Eq. (2). The pre-compensated grating slant angle and period are $\phi_o=\tan^{-1}\left[\tan\phi_s/(1-\delta_v)\right]$ and $\Lambda_o=\Lambda_s\sin\phi_o/\sin\phi_s$ respectively. Where the subscript 'o' and 's' refer respectively to quantities before and after material shrinkage, and δ_v is the shrinkage factor. The measured shrinkage factor δ_v of the DuPont photopolymer HRF-600X123-10 was ~3% after UV fixing processing. The VHGCs are recorded by using a Nd:YAG laser with free-space wavelength λ_w=532nm. The laser beam is spatially filtered and then collimated to obtain a uniform phase-front. The dimensions of the collimated recording beams were 7mm×7mm, and polarized such that the electric field was perpendicular to the plane of incidence (TE-polarization). The index matching oil is inserted between the input prism and substrate, the cover sheet and the output prism. The refractive indices of the photopolymer film are measured using a SPA-4000 Sairon prism coupler. The refractive-indices of the photopolymer film are n_{gw}=~1.51 and n_{gr} =~1.49 at λ_w=532nm and λ_r=1550nm respectively. In addition, the glass substrate material is a fused-silica like that of prisms with refractive index n_{pw}=1.46 and n_{pr}=1.444 at λ_w=532nm and λ_w=1550nm respectively.

With parameters λ_w=532nm, ϕ_s=45°, δ_v=3%, and Λ_s= 0.7355μm, the resulting recording angles in air of Eq. (2) are calculated to be θ_{w1}=26.805° and θ_{w2}=16.999° respectively.

To attain a high contrast ratio of the recording interference pattern through the compensation of the incident powers for the different recording angles, the intensity of the two recording beams are adjusted to be I_{w1}=0.15mW/cm^2 and I_{w2}=0.081mW/cm^2 respectively. Two gratings with same grating periods are written by the use of translation stages, as illustrated in Fig. 2, to set the separation distance between the gratings. After one grating is recorded, the rotation stage with the prism system is then shifted by a translation stages, and the second exposure is made with a same recording angle to form a grating with a same period. The dimensions and the separation length of the fabricated input/output VHGC are ~8.6mm(=L_g)×7mm(=w_g) and 4mm(=Z_L) respectively.

III. EXPERIMENTAL RESULTS

After exposure to the two recording beams, the gratings are fixed by UV light. The fixed sample is then mounted onto a rotation-translation stage in order to test the angular and spectral responses of a fabricated VHGC sample as shown in Fig. 3. A tunable laser which has a center wavelength of 1550nm with a ±30 nm tunable wavelength range is used. The dimensions of the incident laser beam at the surface of the sample were approximately 2 mm(z)×5 mm(y). The polarization of the incident laser beam is controlled by a λ/2 plate and a linear polarizer. Since the VHGC is polarization-sensitive device [12] with strong coupling efficiency for TE polarized light but very weak efficiency for TM polarized light, the TE polarized incident beam was adopted for the experiment. In Fig. 3, the angular tuning is accomplished by rotating the VHGC sample about the y-axis perpendicular to the plane of incidence. In this procedure, angular tuning at a given wavelength leads to a wave-vector mismatch among the grating and the incident and diffracted beams inside the sample, and results in mismatches of a specific waveguide mode. The adjusting procedure for an optimized coupling starts with the first step for tuning a tunable laser to the peak reflectance wavelength for the nearly normal incident input beam. The incident angle is then varied to the coupling angle having a peak reflectance, and then the wavelength is fine-tuned again and the incident angle is fine-tuned around the obtained central values from the first step.

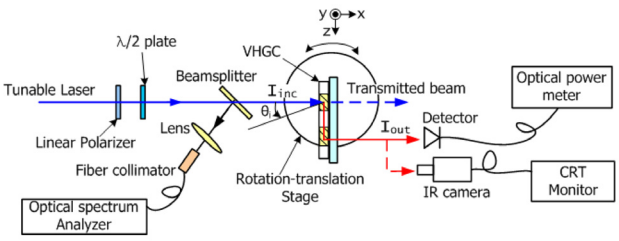

FIG. 3. Experimental setup for testing the fabricated VHGC sample.

Figure 4 shows the angular response of the normalized reflected intensity for a fixed coupling wavelength of 1547.4nm. The TE polarized input beam was positioned at approximately z_o=5mm on the surface of the sample as shown in Fig. 1. We define the output reflectance of the sample as R=(I_{out}/I_{inc}) ×100% in Fig. 3. Where the incident intensity of the input beam I_{inc} defines the intensity of the beam transmitted through the film region without the grating at input coupling angle considering the Fresnel and absorption losses, and I_{out} is the intensity of the deflected output beam from the output coupler.

As seen in Fig. 4, approximately six main TE-modes are excited in the sample, and the shifts in the angular position of the mode curves due to the modal interference are observed. For the fundamental TE_o mode, the measured input coupling angle and output reflectance were θ_c=0.013° and R=6.83%. The higher modes occurs at θ_c=0.266°, 0.533°, 0.739°, 0.826°, 1.226°, and the corresponding R at these coupling angles were 19.44%, 17.89%, 11.12%, 6.61%, 6.46%, respectively. The angular selectivity of TE_1 mode was ~0.033°, which is measured at the half width at first zero (FWFZ) level of the mode curve. Because the VHGC characteristic properties are dominated by the Bragg effect, the angular selectivity inside the $\phi=\pi/4$ slanted volume grating at the FWFZ level can be described theoretically with the Kogelnik formula as $\delta\theta_{FWFZ} \cong \lambda_c \sin\theta_c / n_{gr} t_g \cos 2\theta_c$, where λ_c is the Bragg phase-matched coupling wavelength of the grating, and θ_c is the coupling angle inside the grating [10]. Using the measured values in Fig. 4 with θ_c=0.266° and λ_r=1547.4nm, we obtain an angular selectivity of $\delta\theta_{FWFZ}$=~0.027° for a grating with t_g=10μm. It can be noted that the measured data is only slightly larger than that of the theoretical calculation for a uniform single grating. Furthermore, we investigated the effect of the positions of the incident-beam z_o on the surface of the input VHGC. From the measurement results, the output peak reflectances at the incident-beam positions of z_o=2mm, 5mm, and 7mm are R=17.44%, 19.43%,

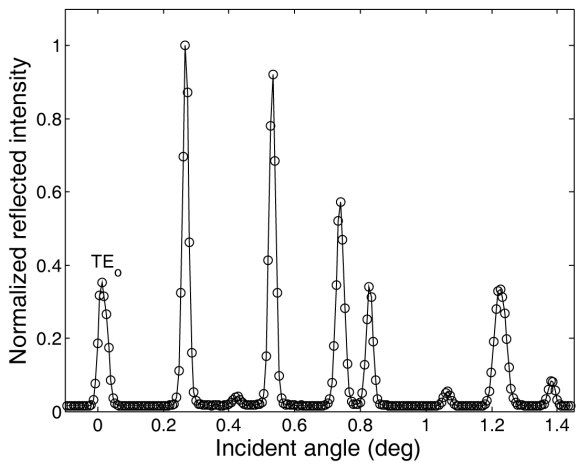

FIG. 4. Normalized reflected intensity versus incident angle for the fabricated input/output VHGC.

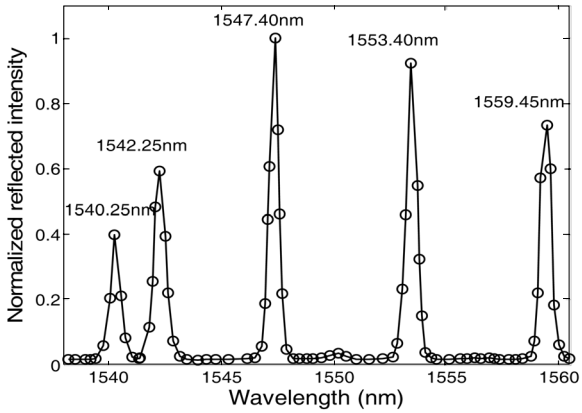

FIG. 5. Normalized reflected intensity versus wavelength for the fixed input coupling angle.

and 34.13%, respectively. This indicates that R increases as the incident-beam position shifts to the grating-waveguide boundary of the input coupler because the out-coupling effect (radiation modes) decrease, whereas the radiation modes are excited by the dephasing due to deviation from the coupling angle. However, as the incident-beam position is increased from z=2 to z=7 mm, the angular selectivity is barely changed. Therefore we are concluding that the input/output VHGC behaves as a single uniform grating, and then the angular selectivity of the input/output VHGC is mainly dependent on the effective thickness of the grating. This is because more light is diffracted from the region closer to the grating-waveguide boundaries (near $z_o=L_g$) and the surface of the grating (near x=0), and thus the grating length L_g does not significantly affect the angular (or wavelength) selectivity [1,3]. Figure 5 shows the spectral response of the normalized reflected intensity as a function of tuning wavelength in the range between 1538.20nm to 1560.45nm for a fixed input coupling angle of a θ_c=0.266° and z_o=5mm. As seen in Fig. 5, approximately five peak reflectance wavelengths are excited in this tuning range, and modal interference can be observed similar to that in Fig. 4 at the central wavelengths with a 1540.25nm and 1542.25nm. A measured wavelength at the FWFZ level is ~0.8nm for a curve centered at 1547.4nm. Using the experimental data θ_c=0.266° and λ_c=1547.4nm in Fig. 4, we estimate approximately the FWFZ wavelength selectivity $\delta\lambda_{FWFZ}$=~0.74nm for a uniform single grating with a 10μm thickness [10]. The measured wavelength-selectivity is also slightly larger than that of the theoretical calculation as the angular selectivity. To better understand the relationship between the coupling angle and coupling wavelength in the waveguide, let us examine the experimental data in Fig. 4 and Fig. 5. If the coupling angle is tuned from the initial alignment angle $\theta_{c,i}$ to the next mode $\theta_{c,i+1}$, then the coupling wavelength of first mode is no longer a coupling wavelength of a next mode. Therefore the wavelength should be changed to satisfy the Bragg-matching condition, the new coupling wavelength

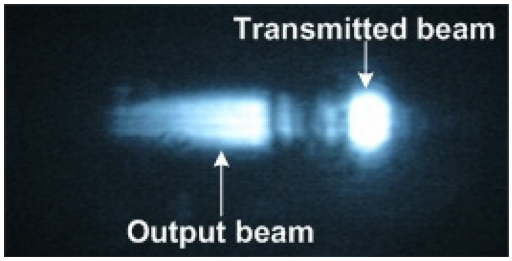

FIG. 6. Photograph of the transmitted and output beam obtained by the IR camera.

$\lambda_{c,i+1}$ can computed from Eq. 1 to be

$$\lambda_{c,i+1} = \lambda_{c,i}\cos(\phi-\theta_{c,i+1})/\cos(\phi-\theta_{c,i}), \quad (3)$$

where we assume that $n_{gr}(\lambda_{c,i})\approx n_{gr}(\lambda_{c,i+1})$ because the angular tuning is limited. The coupling wavelengths of the two adjacent modes in Fig. 5 were $\lambda_{c,i}$=1547.4° and $\lambda_{c,i+1}$= 1553.4° for a fixed coupling angle $\theta_{c,i}$=0.266°. Using these values, the corresponding coupling angle of the $\lambda_{c,i+1}$ mode is expected to be observed to be $\theta_{c,i+1}$=~0.49° from Eq. 3. This value is roughly in accord with the measurement value of 0.533° in Fig. 4. The difference between the calculated value and the measured values is ~0.042°, and this angular difference lead to a ~1.12nm wavelength difference. Also the spacing between the central wavelengths of each mode is not perfectly coincident with the theoretical estimation of Eq. 3. Generally the analytic methods for a common uniform volume grating will not exactly match our experimental results because of the characteristics of a narrow Bragg-selectivity and a wide and thick waveguide in which few modes exist, but it is seen to be still useful to understanding and explaining approximately the behavior of our special configuration.

Figure 6 shows the intensity profile of the output beam coupled out from the output coupler for the incident conditions θ_c=0.266°, λ_c=1547.4nm, and z_o=5mm, where the output beam is captured by using an infrared (IR) camera with a mounted zoom lens in Fig. 3. The intensity profile gradually decreases along the propagation direction z that corresponds to a uniform grating in the output coupling region as shown in Fig. 6.

In our experimental results, the measured input coupling angle and wavelength differ from the design values (θ_c=0° and λ_c=1550nm) and are primarily due to the arrangement errors in optical setups. It is obvious that precision means are necessary to fabricate an input/output VHGC to fulfill the design values within tolerance limits, and guaranteed output performance can be covered by more precise alignment, recording, and testing processes.

IV. CONCLUSIONS

In this paper we have presented design and fabrication

results of a surface-normal input/output VHGC operating at 1550nm wavelength region by using a 10μm-thick DuPont photopolymer HRF600 x 123-10. The angular and wavelength responses of the surface-normal input/output VHGC have been investigated, showing that the input/output VHGC acts as a narrowband input/output coupler, which filters and couples only a spectrally and angularly narrow portion of the light. The angular and wavelength selectivity is mainly dependent on the effective thickness of the grating, which is consistent with the behavior of volume gratings in bulk diffraction, where thicker gratings cause narrower angular and wavelength selectivity. The output reflectance increases as the incident-beam position closes toward the grating-waveguide boundary of the input coupler, but the angular selectivity is barely changed. Our experimental results will be useful examples for understanding the behavior of the input/output VHGC embedded in a waveguide configuration and applications as the devices for integrated optics and WDM optical communications.

ACKNOWLEDGMENT

This research was supported by Basic Science Research Program through the National Research Foundation of Korea (NRF) funded by the Ministry of Education, Science and Technology (2009-0072569)

REFERENCES

1. M. L. Jones, R. P. Kenan, and C. M. Verber, "Rectangular characteristic gratings for waveguide input and output coupling," Appl. Opt. **34**, 4149-4158 (1995).
2. S. D. Wu and E. N. Glytsis, "Volume holographic grating couplers: rigorous analysis by use of the finite-difference frequency-domain method," Appl. Opt. **43**, 1009-1023 (2004).
3. S. D. Wu, E. N. Glytsis, and T. K. Gaylord, "Optimization of finite-length input volume holographic grating couplers illuminated by finite-width incident beams," Appl. Opt. **44**, 4435-4446 (2005).
4. A. H. Phan, N. Kim, J. H. Park, and K. Y. Lee, "Input-output coupler system with 45-degree slant angle based on Bragg hologram," J. Opt. Soc. Korea **13**, 123-130 (2009).
5. A. H. Phan, D. D. Do, N. Kim, J. H. Park, and K. Y. Lee, "Input-output coupler working at a1550nm wavelength using multi-holographic Bragg gratings," in *Proc. IEEE International Conference on Advanced Technologies for Communications* (Hanoi, Vietnam, Oct. 2008), pp. 132-135.
6. R. A. Villalaz E. N. Glytsis, T. K. Gaylord, and T. Nakai, "Wavelength response of waveguide volume grating couplers for optical interconnects," Appl. Opt. **43**, 5162-5167 (2004).
7. W. Driemeier, "Bragg-effect grating couplers integrated in multicomponent polymeric waveguides," Opt. Lett. **15**, 725-727 (1990).
8. Q. Huang and P. Ashley, "Holographic Bragg grating input-output couplers for polymer waveguides at an 850-nm wavelength," Appl. Opt. **36**, 1198-1203 (1997).
9. S. M. Schultz, E. N. Glytsis, and T. K. Gaylord, "Design, fabrication, and performance of preferential-order volume grating waveguide couplers," Appl. Opt. **39**, 1223-1232 (2000).
10. H. Kogelnik, "Coupled wave theory for thick hologram gratings," Bell Syst. Tech. J. **48**, 2909-2947 (1969).
11. C. Zhao, J. Liu, Z. Fu, and R. T. Chen, "Shrinkage correction of volume phase holograms for optical interconnects," Proc. SPIE **3005**, 224-229 (1997).
12. H. Kogelnik and T. P. Sosnowski, "Holographic thin film couplers," Bell Syst. Tech. J. **49**, 1602-1608 (1970).